The Crop Journal 9 (2021) 372–379

Contents lists available at ScienceDirect

The Crop Journal

journal homepage: www.elsevier.com/locate/cj

Mapping QTL for flowering time-related traits under three plant densities in maize

Liwei Wang [a,b], Zhiqiang Zhou [b], Ronggai Li [a], Jianfeng Weng [b], Quanguo Zhang [a], Xinghua Li [a], Baoqiang Wang [a], Wenying Zhang [a], Wei Song [a,*], Xinhai Li [b,*]

[a] The Key Laboratory of Crop Genetics and Breeding of Hebei Province, Institute of Cereal and Oil Crops, Hebei Academy of Agriculture and Forestry Sciences, Shijiazhuang 050035, Hebei, China
[b] Institute of Crop Sciences, Chinese Academy of Agricultural Sciences, Beijing 100081, China

ARTICLE INFO

Article history:
Received 25 December 2019
Revised 12 June 2020
Accepted 23 September 2020
Available online 17 November 2020

Keywords:
Maize
Flowering time
Plant density
Recombinant inbred lines (RIL)
Genetic basis

ABSTRACT

Flowering time is an indicator of adaptation in maize and a key trait for selection in breeding. The genetic basis of flowering time in maize, especially in response to plant density, remains unclear. The objective of this study was to identify maize quantitative trait loci (QTL) associated with flowering time-related traits that are stably expressed under several plant densities and show additive effects that vary with plant density. Three hundred recombinant inbred lines (RIL) derived from a cross between Ye 478 and Qi 319, together with their parents, were planted at three plant densities (90,000, 120,000, and 150,000 plants ha^{-1}) in four environments. The five traits investigated were days to tasseling (DTT), days to silking (DTS), days to pollen shed (DTP), interval between anthesis and silking (ASI), and interval between tasseling and anthesis (TAI). A high-resolution bin map was used for QTL mapping. In the RIL population, the DTT, DTS, and DTP values increased with plant density, whereas the ASI and TAI values showed negligible response to plant density. A total of 72 QTL were identified for flowering time-related traits, including 15 stably expressed across environments. Maize flowering time under different densities seems to be regulated by complex pathways rather than by several major genes or an independent pathway. The effects of some stable QTL, especially *qDTT8-1* and *qDTT10-4*, varied with plant density. Fine mapping and cloning of these QTL will shed light on the mechanism of flowering time and assist in breeding early-maturing maize inbred lines and hybrids.

1. Introduction

Maize (*Zea mays* L.) is a major global source of food, forage, and bioenergy [1]. Maize also is one of the most adaptable crops [2]. Numerous landraces and commercial hybrids show features such as flowering time, maturity, and plant architecture that are adapted to various climates and locations. Flowering time is a key breeding target of maize because it reflects adaptability to a given environment and varies among agro-ecological zones with different farming systems [3,4]. For example, a winter wheat–summer maize rotation is a dominant farming system in the Huang-Huai-Hai plain, a major maize production area in northern China, whereas a single maize crop per year is the typical mode for grain production in northeastern China.

Flowering time has been widely investigated in numerous plant species, especially in *Arabidopsis thaliana* and rice (*Oryza sativa*) [5,6]. Hundreds of genes that control flowering time have been identified in *Arabidopsis* and a relatively complete flowering-time gene regulatory network has been constructed for this species [7–9]. In contrast, our understanding of the genetic mechanisms of flowering time in maize is still rudimentary. Several genes affecting flowering time have been cloned in maize using comparative genomics, such as *ZmCCA1* [10], *ZmMADS1* [11], and *ZmCOL3* [12], which are homologous to *AtCCA1* and *AtSOC1* in *Arabidopsis* and to *OsCOL4* in rice. Overexpression of any of these genes delayed flowering time in maize or *Arabidopsis*. Only a handful of flowering time mutants in maize have been reported to date. For example, the *gigantea1* (*gi1*) mutant promotes flowering earlier than wild-type under long day condition, while *delayed flowering1* (*dlf1*), *indeterminate1* (*id1*), and *leafy* (irrelevant to *Arabidopsis LFY*) are all late-flowering mutants [13–16]. Among these, *DLF1* and *ID1* have been cloned [14,15]. *DLF1* is a homolog of *Arabidopsis FLOWERING*

* Corresponding authors.
E-mail addresses: sw1717@126.com (W. Song), lixinhai@caas.cn (X. Li).

https://doi.org/10.1016/j.cj.2020.07.009

LOCUS D (*FD*) and encodes a bZIP transcription factor [14]. The *ID1* gene appears to be present only in grasses, as no homologs of this gene are present in *Arabidopsis*, implying divergence in the genetic basis of flowering time between monocots and dicots, and encodes a zinc-finger transcription factor [7,15]. Flowering time in maize is controlled by a set of small-effect QTL [2], and several QTL have been identified using large populations, such as RIL and NAM populations, and high-resolution genetic linkage maps [2,7,17,18]. Only a few genes controlling flowering time have been fine-mapped or cloned, including *Vgt1* (*Vegetative to generative 1*) [19], *ZCN8* [3], *ZmMADS69* [20], *ZmCCT9* [4], and *ZmCCT* [21,22].

The per-plant yield potential of maize has reached an apparent plateau with the use of maize hybrids, and the more gradual increases in maize yield in recent decades have been attributed primarily to tolerance of high plant density [23–26]. However, high plant density may result in delayed flowering time and late maturity [23,27]. The genetic architecture of maize flowering time under high plant density has been less studied than yield-related traits. For instance, under 52,500 and 90,000 plants ha^{-1}, Guo et al. [24] found that decreases of partial yield-component traits under high density could be compensated by increased plant number, and 76 QTL were associated with the 10 yield-related traits; Ma et al. [28] identified four heterosis-related genes in maize under two plant densities (45,000 and 67,500 plants ha^{-1}).

The objective of the present study was to identify stable and density-specific QTL for flowering-time-related traits in 300 maize recombinant inbred lines planted at three densities. The present study aims to broaden our understanding of the genetic basis of flowering time under high plant densities and improve the theoretical basis for molecular marker-assisted breeding in maize.

2. Materials and methods

2.1. Materials

A population of 300 recombinant inbred lines (RIL) was randomly selected from a set of 365 RIL derived from a cross between Ye 478 (PA heterotic group) and Qi 319 (PB heterotic group) by single-seed descent. The RIL population and parents grown at 60,000 plants ha^{-1} have been described [17,29,30]. The 365 RIL had been genotyped with 86,257 single nucleotide polymorphism (SNPs), and a high-resolution linkage map with 4602 bin markers was constructed [17,29]. The total genetic length of the map was 1533.72 cM with a mean genetic distance of 0.33 cM, equivalent to a physical distance of 0.45 Mb, between adjacent markers [17,29].

2.2. Field trials and phenotyping

Phenotypes were evaluated in two locations per year in the 2017 and 2018 summer maize seasons. Three plant densities were employed in each location: 90,000 (low plant density, LPD), 120,000 (moderate plant density, MPD), and 150,000 plants ha^{-1} (high plant density, HPD). In Shijiazhuang, Hebei province (37.27°N, 113.30°E), all RIL and their parents were sown on June 18, 2017 and June 14, 2018. In Xinxiang, Henan province (35.19°N, 113.53°E), the materials were sown on June 20, 2017 and June 16, 2018. Field trials were laid out in randomized complete blocks with three replications. Each line was grown in a single 4-m row, with 0.6-m row spacing. Field management followed local production practice.

Three primary and two secondary flowering time-related traits were measured: days to tasseling (DTT, number of days from sowing to tasseling of 50% plants), days to silking (DTS, number of days from sowing to silking of 50% plants), days to pollen shed (DTP, number of days from sowing to top third of the tassels shedding pollen), anthesis–silking interval (ASI = DTP − DTS), and tasseling–anthesis interval (TAI = DTP − DTT).

2.3. Statistical analysis

The mean of three replications in each environment was used as a measurement. Analysis of variance (ANOVA), correlation analysis and broad-sense heritability (H^2) calculation were performed with SPSS version 22 [31]. To reduce the influence of external factors on phenotypic variation, a BLUE (best linear unbiased estimate) value for each recombinant inbred line at each plant density was calculated using QTL IciMapping 4.1 software [32]. The H^2 value was estimated as follows [33]:

$$H^2 = \frac{\sigma_G^2}{\sigma_G^2 + \frac{\sigma_{GE}^2}{n} + \frac{\sigma^2}{nr}} \quad (1)$$

where σ_G^2 is genotypic variance, σ_{GE}^2 is the effect of interaction between genotype and environment, σ^2 is error variance, n is the number of environments, and r is the number of replications in each environment.

2.4. QTL mapping

QTL were identified using the inclusive composite interval mapping (ICIM) method in QTL IciMapping with the scanning step and PIN value of 0.1 cM and 0.0002, respectively. The LOD (logarithm of odds) score for declaring a significant QTL was estimated as 3.3 using 1000 permutations and *P*-value of 0.05 [32,34]. For single-environment QTL mapping analysis, phenotypic data consisted of means of three replications in a single environment. For single-plant density QTL mapping analysis, phenotypic data consisted of BLUE values across environments at a given plant density. QTL for a given trait with the same or overlapping confidence intervals were considered to be a single QTL, and QTL for different traits with the same or overlapping confidence intervals were considered to be a QTL cluster or a pleiotropic QTL. In particular, QTL identified at all three plant densities were considered to be stable QTL. Location-specific QTL were defined as QTL identified in only one location and density-specific QTL as QTL identified only under one plant density.

3. Results

3.1. Phenotypic evaluation of five traits related to flowering time under three plant densities

Among the five traits, there was no significant difference between the parents Ye 478 and Qi 319 in DTT, whereas the phenotypic values of DTS, DTP, and TAI were higher for Ye 478 than for Qi 319, and those of ASI were higher for Qi 319 than for Ye 478 (Table 1; Table S1). The values of all five traits in the two parents increased with plant density. In the RIL population, the phenotypic values of the primary traits DTT, DTS, and DTP also increased with plant density. However, the phenotypic values of the secondary traits ASI and TAI were insensitive to plant density (Table 1; Table S1). Bidirectional transgressive segregation of all traits was observed in all measured environments, suggesting that these traits are quantitative traits under polygenic control and the genetic difference of flowering time exist in in the parental lines. All five traits showed high broad-sense heritability (H^2) across all environments, ranging from 69.68% (TAI in E9) to 96.43% (DTP in E4). The broad-sense heritability of the primary flowering time-related traits was higher than that of the secondary traits, indicat-

Table 1
Descriptive statistics for flowering time-related traits of the parental lines and RIL population under three plant densities using BLUE values.

Trait	Plant density	Ye 478	Qi 319	RIL population					
				Mean ± SD	Range	Skewness	Kurtosis	CV (%)	H^2 (%)
DTT	LPD	54.36	54.33	54.54 ± 1.73	49.71–61.00	0.24	0.94	3.17	82.08
	MPD	55.37	55.47	55.03 ± 1.82	50.00–61.50	0.29	1.09	3.31	80.88
	HPD	56.04	56.25	55.53 ± 1.53	51.50–61.33	0.39	0.46	2.76	78.58
DTS	LPD	59.83	58.92	59.06 ± 2.41	53.00–68.00	0.35	0.49	4.08	82.49
	MPD	59.66	59.68	59.77 ± 2.37	54.07–68.00	0.10	0.25	3.97	80.3
	HPD	61.21	60.94	60.19 ± 2.17	54.50–66.50	0.41	0.30	3.61	79.2
DTP	LPD	57.25	56.6	58.70 ± 2.18	53.50–64.91	0.29	0.06	3.71	83.15
	MPD	61.24	59.14	59.11 ± 2.22	53.21–65.00	0.15	0.05	3.76	83.22
	HPD	60.53	59.54	59.79 ± 2.05	55.06–66.00	0.41	0.24	3.43	79.25
ASI	LPD	−0.41	−0.6	0.53 ± 1.41	−3.65–5.27	0.17	0.31	266.04	79.51
	MPD	0.66	1.96	0.50 ± 1.42	−3.50–5.15	0.25	0.04	284.00	75.48
	HPD	1.18	2.24	0.58 ± 1.44	−3.50–4.27	−0.02	−0.23	248.28	76.55
TAI	LPD	3.63	2.58	3.96 ± 1.02	1.00–7.50	0.37	0.19	25.76	73.51
	MPD	4.52	2.41	3.99 ± 1.04	1.76–8.00	0.76	0.75	26.07	71.13
	HPD	4.21	2.78	4.02 ± 1.00	1.87–7.00	0.44	−0.09	24.88	67.48

DTT, days to tasseling; DTS, days to silking; DTP, days to pollen shed; ASI, anthesis–silking interval; TAI, tasseling–anthesis interval; LPD, low plant density (90,000 plants ha^{-1}); MPD, moderate plant density (120,000 plants ha^{-1}); HPD, high plant-density (150,000 plants ha^{-1}); BLUE, best linear unbiased estimate; SD, standard deviation; CV (%), coefficient of variation; H^2 (%), broad-sense heritability.

ing that stably inherited genetic factors played crucial roles in the establishment of these traits (Table 1; Table S1).

Heat maps of the phenotypic data in the 12 environments revealed high correlations among the five traits, suggesting that use of the BLUE values for the five traits was suitable for statistical analyses and QTL mapping (Fig. S1). Highly significant ($P < 0.001$) differences were found among genotypes, environments, and G × E interactions for all traits (Table S2). There were significant positive correlations among DTT, DTS, and DTP (Fig. 1). Similarly to DTP and TAI, DTS showed a low positive correlation with ASI. There was a weak negative correlation between ASI and TAI. No correlations were detected between the other traits. The correlations among the five traits were little affected by plant density (Fig. 1).

3.2. QTL mapping of flowering time-related traits in the RIL population

QTL for the five traits were detected across all 12 individual environments under each of three plant densities.

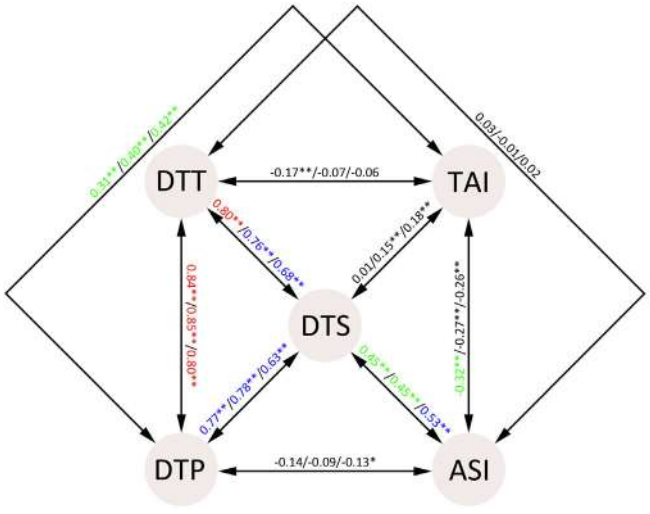

Fig. 1. Significant correlations for flowering time-related traits in the RIL population under three plant densities. The numbers represent Pearson correlation coefficients between traits under LPD, MPD and HPD, and the red, blue, green, and black numbers indicate respectively high, moderate, low, or no correlation; single and double asterisks indicate significance at $P < 0.05$ and $P < 0.01$, respectively.

3.2.1. DTT

A total of 15 QTL influencing DTT, distributed on all chromosomes except 4, 6, and 9, were identified by single-environment mapping (Fig. 2; Table S3). The individual QTL contributions to phenotypic variance ranged from 3.90% (*qDTT2* in E7) to 17.80% (*qDTT10-2* in E1) and the cumulative contributions from 15.62% (E8) to 38.13% (E9; Table S4). Nine QTL were detected under at least two plant densities. *qDTT5* on chromosome 5 was a plant density-specific QTL identified only in LPD in 2018, explaining 5.08%–6.15% of the phenotypic variation in DTT. The six stable QTL *qDTT3-1*, *qDTT7-2*, *qDTT10-2*, *qDTT2*, *qDTT10-4*, and *qDTT8-1* were detected in respectively four, four, five, seven, eight, and nine environments under all three plant densities. Three location-specific QTL, *qDTT10-2* (Shijiazhuang), *qDTT1-1* (Xinxiang), and *qDTT1-4* (Xinxiang), all showed positive additive effects and were detected under at least two plant densities, and indicated that they carry alleles derived from parent Qi 319 that could delay tasseling. The stable QTL *qDTT2* was detected in seven environments and contributed 3.90%–10.70% of the phenotypic variation in DTT. The additive effects of this QTL ranged from − 0.25 to − 0.54, implying that the *qDTT2* allele from Qi 319 promoted tasseling. A QTL with positive additive effects, *qDTT10-4*, was consistently detected in eight environments under all plant densities and explained 4.09%–9.67% of the phenotypic variation in DTT. The mapped locations of another stable QTL, *qDTT8-1* overlapped in bin 8.02 on chromosome 8 in nine different environments. *qDTT8-1* explained 4.10%–9.88% of the phenotypic variation in DTT and the allele derived from Qi 319 advanced tasseling by 0.25–0.60 days. The effects of *qDTT8-1* with increasing plant density appeared to be cumulative (Table S5).

3.2.2. DTS

Twelve QTL for DTS were discovered in single environments, with nine QTL were detected uniquely in Xinxiang (Fig. 2; Table S3). The mapped locations of five QTL, including three location-specific QTL, *qDTS1-2* (Xinxiang), *qDTS2-2* (Xinxiang), and *qDTS2-3* (Shijiazhuang), overlapped under two plant densities. *qDTS3-1* and *qDTS9* showed opposite additive effects on DTS and were identified uniquely in Xinxiang under all three plant densities. *qDTS7* and *qDTS10* both showed positive additive effects on DTS and were identified under two plant densities. No QTL explained more than 10% of the phenotypic variation in DTS, suggesting that DTS is controlled by a set of small-effect QTL (Table S3).

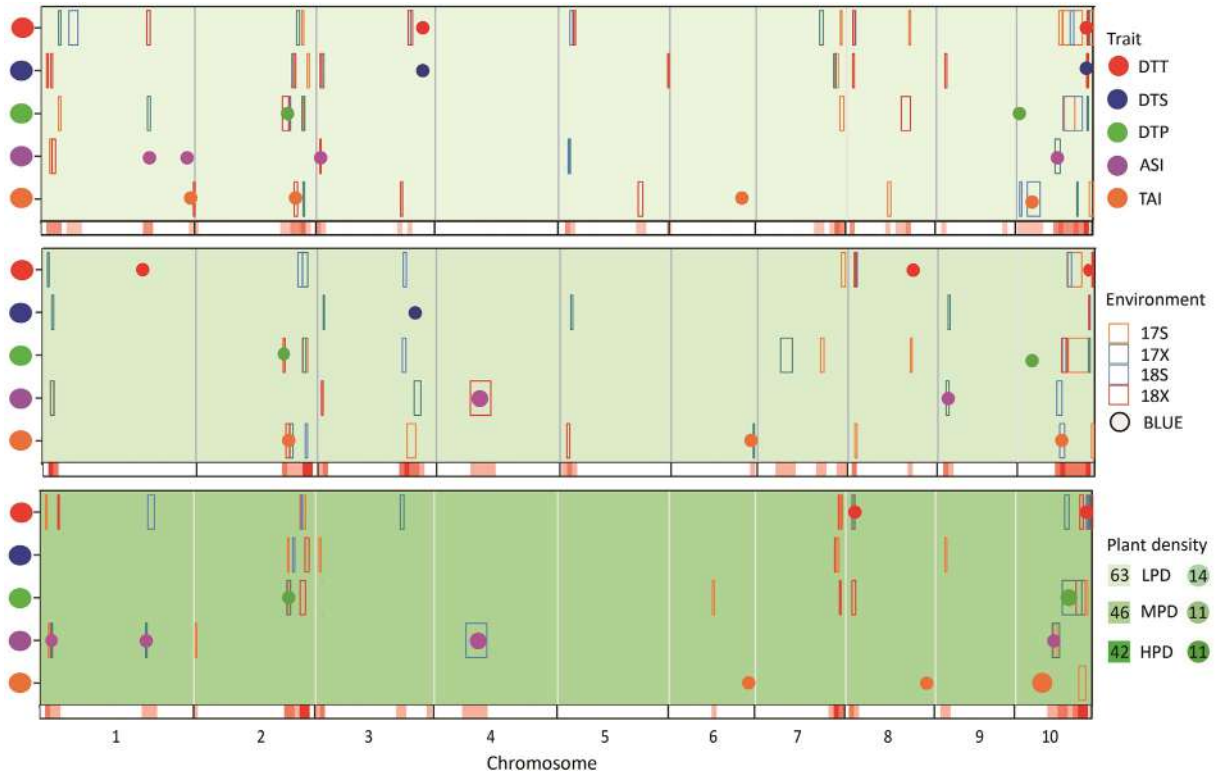

Fig. 2. Chromosomal distribution of quantitative trait loci (QTL) identified for flowering time-related traits in maize. QTL regions for flowering time-related traits represented by confidence intervals are shown as boxes (for single-environment analysis) or circles (for BLUE analysis), and the colors of these boxes indicates the respective environment. The width of each box or circle reflects the length of the confidence interval. The top, middle and bottom parts of the figure represent low plant density (LPD, 90,000 plants ha^{-1}), moderate plant density (MPD, 120,000 plants ha^{-1}), and high plant density (HPD, 150,000 plants ha^{-1}), respectively. The red, blue, green, purple, and orange circles at left represent QTL for DTT, DTS, DTP, ASI, and TAI, respectively. 17S, 17X, 18S, and 18X represent 2017 Shijiazhuang, 2017 Xinxiang, 2018 Shijiazhuang, and 2018 Xinxiang, respectively.

3.2.3. DTP

Fifteen QTL influencing DTP were detected in all single environments, but only six of them were expressed under at least two plant densities (Fig. 2; Table S3). One plant density-specific QTL, *qDTP10-2*, was detected only under MPD in 2018 and explained 6.46%–14.35% of the phenotypic variation in DTP. Three location-specific QTL were identified, including *qDTP7-3* in Shijiazhuang, *qDTP10-3* in Shijiazhuang, and *qDTP10-5* in Xinxiang. The stable QTL *qDTP10-5* explained 4.76%–11.98% of the phenotypic variation. The major QTL *qDTP10-4* was revealed on one environment (E9) in which it explained 10.84% of the phenotypic variation in DTP. Another major QTL located on chromosome 10, *qDTP10-3*, was expressed repeatedly under all three plant densities. *qDTP10-3* explained 9.89%–15.33% of the phenotypic variation in DTP and the Qi 319 allele delayed DTP up to 1.03 days. Two stable QTL on chromosome 2, *qDTP2-1* and *qDTP2-2*, both showed negative additive effects, indicating that their alleles were derived from parent Qi 319 and promoted pollen shedding. The additive effect of *qDTP2-1* diminished with increasing plant density (Table S5).

3.2.4. ASI

ASI was governed by nine QTL located on chromosomes 1, 2, 3, 4, 5, 9, and 10, and four of these QTL were detected in single environments (Fig. 2; Table S3). The mapped locations of the plant density-specific QTL *qASI5* overlapped in two environments under LPD and they had positive additive effects. The location-specific QTL *qASI3-1* (Xinxiang) and *qASI4* (Xinxiang) displayed opposite additive effects and explained up to 16.10% and 13.95%, respectively, of the phenotypic variation. The stable QTL with negative additive effects *qASI1-1* and *qASI10* were repeatedly identified in seven and four environments, respectively. *qASI1-1* explained from 5.82% to 10.58% and *qASI10* explained 5.87%–9.28% of the phenotypic variation. Interestingly, the stable QTL *qASI1-1* was consistently identified under all three plant densities, its maximum LOD scores and the proportions of phenotypic variation explained were both highest under HPD, and the Qi 319 allele reduced ASI by up to 0.54 days (Table S5).

3.2.5. TAI

Fourteen QTL influencing TAI were identified in 12 environments and 10 of them were detected in only a single environment or plant density (Fig. 2; Table S3). Five QTL including *qTAI2-1*, *qTAI2-2*, *qTAI3*, *qTAI10-5*, and *qTAI10-6* were detected under two plant densities and three of these QTL were location-specific, excluding *qTAI2-2* and *qTAI3*. However, no stable QTL for TAI were identified during single-environment mapping. Five QTL influencing TAI were identified on chromosome 10. Two major QTL on chromosome 10 were both identified in different individual environments. *qTAI10-2* explained 16.11% of the phenotypic variation in E3 and *qTAI10-4* explained 14.66% in E7. *qTAI10-2* and *qTAI10-4* contributed additive effects to TAI of respectively 0.55 and 0.57 day. *qTAI2-1*, *qTAI2-2*, and *qTAI6* contributed negative additive effects, showing that the alleles increasing TAI were derived from parent Ye 478.

In all, 65 QTL for flowering time-related traits were detected on all 10 maize chromosomes across 12 individual environments under three plant densities. These included 42 QTL for primary and 23 QTL for secondary traits (Fig. 2; Table S3). The phenotypic variation explained by individual QTL ranged from 3.70% (*qDTS8* in E4) to 17.80% (*qDTT10-2* in E1) and total cumulative contribu-

tions of these QTL for each trait were 5.84% (ASI in E1) to 38.13% (DTT in E9) in each environment (Table S4). Among these QTL, 35 were identified in only a single environment, 16 were discovered under two plant densities, 14 were detected as stable QTL, and three were identified as plant density-specific QTL. Of 16 location-specific QTL, five were stable QTL and the remaining 11 were each identified under two plant densities.

3.3. QTL detection using BLUE values

In total, 25 QTL were identified for all the flowering time-related traits across all 10 chromosomes using BLUE values (Fig. 2; Table S6). Of these, five, two, four, seven, and seven QTL were detected for DTT, DTS, DTP, ASI, and TAI, respectively. The maximum of eight QTL were identified on chromosome 10, followed by five QTL on chromosome 1. Three QTL were identified on chromosomes 2, 3, and 8. Only one QTL was identified on each of chromosomes 4, 6, and 9 (Table S6). A total of 18 QTL overlapped with other corresponding QTL in single-environment mapping and seven QTL were uniquely identified using BLUE values (Fig. 2; Tables S3 and S6). All the QTL detected using BLUE values were small-effect QTL, among which none explained more than 10% of the phenotypic variation in a trait and the total phenotypic variance of QTL for any trait ranged from 3.97% (DTS in MPD) to 23.68% (ASI in LPD) at each plant density (Tables S4 and S6). Low levels of phenotypic variation for some traits may be the reason some of these QTL could not be identified by single-environment analysis. A total of 16 QTL were detected at only one plant density, while seven QTL were discovered under two plant densities and two stable QTL were repeatedly identified under all three plant densities. Each of the two stable QTL, *qDTT10-4*, and *qTAI6*, were also identified at some plant densities by single-environment analysis and the additive effects of *qDTP10-4* increased with plant density (Tables S3, S5 and S6).

3.4. Clusters of colocalized QTL associated with flowering time-related traits

The 72 QTL identified in this study by single-environment analysis and single-plant density analysis included 21 sets of overlapping QTL (Tables S3 and S6). These 21 QTL clusters (QCs) comprising 57 QTL were distributed on all chromosomes except for chromosomes 4 and 6. The cloned genes *ZCN8* and *ZmCCT* were included in QC15 and QC19, respectively (Fig. 3; Table 2). The highest number of QCs was five each on chromosomes 1 and 10; followed by three on chromosome 3; two QCs on each of chromosomes 2, 7, and 8; and one QC on each of chromosomes 5 and 9. Eleven clusters of co-located QTL for two traits were mapped to chromosomes 1, 3, 7, 8, 9, and 10. Five clusters on chromosomes 1, 2, 3, 7, and 10 included QTL for three traits. Although five hotspots on chromosomes 2 (bins 2.07–2.08), 5 (bin 5.03), 8 (bin 8.02), 10 (bin 10.03), and 10 (bins 10.05–10.07) included QTL for four traits, no individual clusters harbored QTL for all five traits. A total of 11 QCs contained QTL for DTT and DTP, indicating that

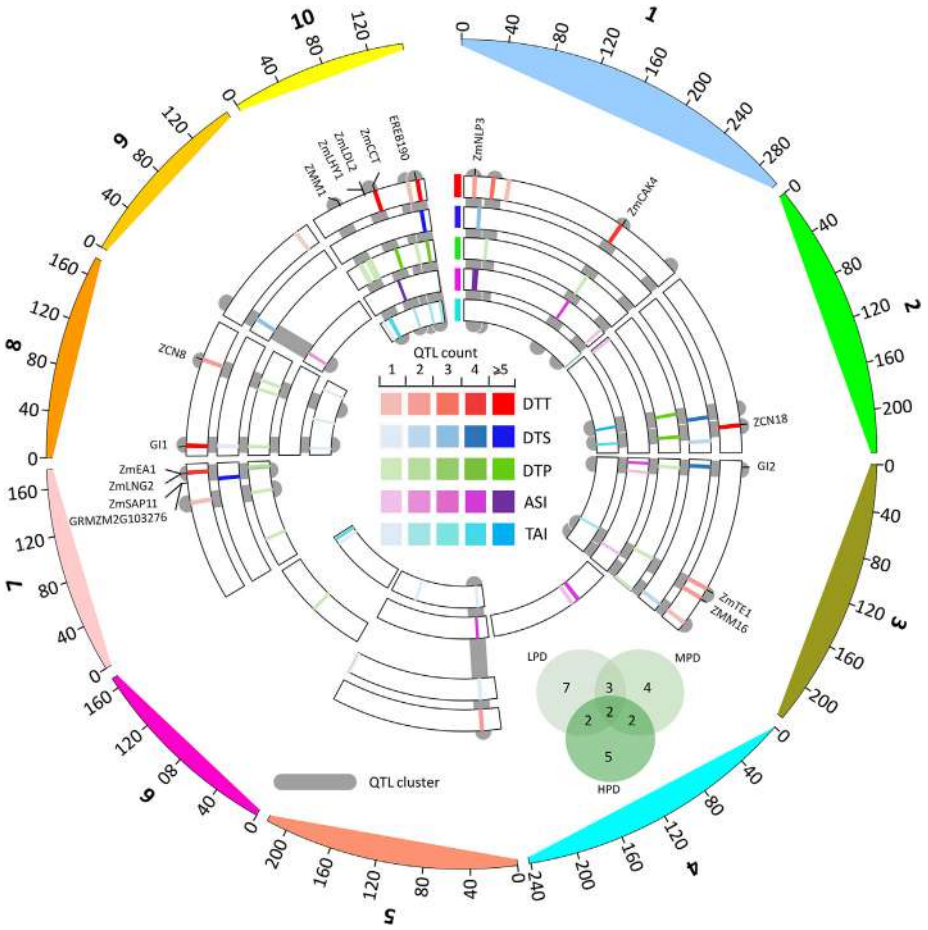

Fig. 3. Genomic distribution of QTL clusters (QCs) for flowering time-related traits and associated flowering time genes. The outmost layer represents the lengths (Mb) of the 10 chromosomes of maize. The different colors indicate different traits: DTT (red), DTS (blue), DTP (green), ASI (purple), and TAI (cyan). A series of color gradients indicate the frequency at which a given QTL was identified in different environments. The distribution of QTL detected using BLUE values is depicted as a Venn diagram.

Table 2
QTL clusters identified for flowering time-related traits.

QTL cluster	Chr.	Interval (Mb)	Physical length (Mb)	Bin	No. of QTL	Integrated QTL	Associated gene
QC1	1	11.35–11.65	0.30	1.01	2	*qDTT1-1*, *qDTS1-1*	
QC2	1	16.95–23.10	6.15	1.02	2	*qDTS1-2*, *qASI1-1*	*ZmNLP3*
QC3	1	34.90–35.95	1.05	1.03	2	*qDTT1-2*, *qDTP1-1*	
QC4	1	207.75–216.55	8.80	1.07	3	*qDTT1-4*, *qDTP1-2*, *qASI1-2*	*ZmCKA4*
QC5	1	289.35–300.60	11.25	1.12	2	*qASI1-3*, *qTAI1*	
QC6	2	171.10–187.55	16.45	2.06–2.07	3	*qDTS2-1*, *qDTP2-1*, *qTAI2-1*	
QC7	2	190.40–214.90	24.50	2.07–2.08	4	*qDTT2*, *qDTS2-2*, *qDTP2-2*, *qTAI2-2*	*ZCN18*
QC8	3	7.15–11.85	4.70	3.02–3.03	2	*qDTS3-1*, *qASI3-1*	*GI2*
QC9	3	165.40–181.70	16.30	3.05–3.06	3	*qDTT3-1*, *qDTP3-2*, *qTAI3*	*ZmTE1*, *ZMM16*
QC10	3	217.90–227.25	9.35	3.09	2	*qDTT3-2*, *qDTS3-2*	
QC11	5	13.30–29.85	16.55	5.03	4	*qDTT5*, *qDTS5-1*, *qASI5*, *qTAI5-1*	
QC12	7	123.45–125.45	2.00	7.02	2	*qDTT7-1*, *qDTP7-2*	
QC13	7	152.05–165.65	13.60	7.03–7.04	3	*qDTT7-2*, *qDTS7*, *qDTP7-3*	*ZmEA1*, *ZmSAP11*, *ZmLNG2*, *GRMZM2G103276*
QC14	8	10.95–21.10	10.15	8.02	4	*qDTT8-1*, *qDTS8*, *qDTP8-1*, *qTAI8-1*	*GI1*
QC15	8	107.40–122.55	15.15	8.03–8.04	2	*qDTT8-2*, *qDTP8-2*	*ZCN8*
QC16	9	16.20–20.55	4.35	9.02	2	*qDTS9*, *qASI9*	
QC17	10	21.05–43.85	22.80	10.03	2	*qDTP10-1*, *qTAI10-2*	*ZMM1*
QC18	10	70.80–87.15	16.35	10.03	4	*qDTT10-1*, *qDTP10-2*, *qASI10*, *qTAI10-4*	*ZmLHY1*, *ZmLDL2*
QC19	10	91.25–106.10	14.85	10.04	2	*qDTT10-2*, *qDTP10-3*	*ZmCCT*
QC20	10	118.45–126.95	8.5	10.04	3	*qDTT10-3*, *qDTP10-4*, *qTAI10-5*	
QC21	10	137.25–145.65	8.40	10.05–10.07	4	*qDTT10-4*, *qDTS10*, *qDTP10-5*, *qTAI10-6*	*EREB190*

these two traits share a genetic basis. QC9 and QC20 harbored QTL for DTT, DTP, and TAI. No QC co-localized QTL influencing DTS, DTP, and ASI.

4. Discussion

The control of flowering time has been intensively investigated in various cereals including rice, wheat, and barley, as it is closely related to agronomic parameters including harvest time, biomass yield, crop rotation patterns, and terminal drought avoidance [5,35–37]. However, the genetic basis of flowering time is not yet completely understood in maize. The majority of QTL we identified were small-effect QTL and no QTL for DTS explained more than 10% of the phenotypic variation (Tables S3 and S6). Our results confirmed previous [2,7] findings that many small-effect QTL control flowering time in maize. Although several QTL affecting flowering time in maize have been reported, only a few of these QTL have yet been fine mapped and cloned [2–4,7,18–22]. Most of the genetic analyses of flowering time in maize have been performed under the typical plant density of about 60,000 plants ha^{-1}. Thus, our results under high plant densities could enrich our understanding of the genetic mechanisms of flowering time in maize.

The phenotypic values for the timing of DTT, DTS, and DTP were all delayed with increasing plant density, while ASI and TAI were insensitive to plant density, as found in previous studies [23,25–27]. The prolongation of the time to reach maturity under higher plant density might thus delay the transition from vegetative to reproductive stage. Although there were relatively small differences in phenotypic values between the parental lines Ye 478 and Qi 319, bidirectional transgressive segregation of these five flowering time-related traits in the RIL population was observed in all environments (Table 1; Table S1). We identified 15, 12, 15, 9, and 14 QTL for DTT, DTS, DTP, ASI, and TAI, respectively, by single-environment analysis (Table S3). We observed high broad-sense heritabilities and correlations for these five traits in all environments (Table 1; Tables S1 and S2; Fig. S1). We thus used the BLUE values to reduce the effects of genotype × environment interactions (G × E) and finally identified 25 QTL for all five flowering time-related traits (Table S6). All of these 25 QTL were small-effect QTL and 18 were identified repeatedly by single-environment analysis (Fig. 2; Tables S3 and S6). Finally, we identified a total of 72 QTL, more than half of which were uniquely identified in an individual environment.

We identified 15 stable QTL under all three plant densities tested, suggesting that the genetic basis of maize flowering time is partially consistent under different plant densities (Table 2; Tables S3 and S6). The additive effects of four of these QTL increased with plant density (Table S5). Although three of these four QTL had negative additive effects, the decrease in DTP influenced by *qDTP2-1* with increasing plant density was opposite to of the trends observed for traits influenced by *qDTT8-1* and *qASI1-1*. *qDTT10-4*, with the positive additive effect, was identified in both single-environment and single-plant density analysis as a stable QTL. Its additive effects increased gradually with plant density as well. These observations suggest that the four QTL, especially *qDTT8-1* and *qDTT10-4*, will be of great practical value for breeding maize inbred lines and commercial hybrids with tolerance to high plant density. We also identified 16 location-specific QTL and three plant density-specific QTL. For example, *qDTS10* was identified under LPD and MPD using single-environment analysis and under LPD using single-plant density analysis. These results suggest that flowering time in maize is influenced by various genetic mechanisms or that QTL for flowering time are selectively expressed under specific plant densities (Table 2; Table S6).

Although flowering time-related QTL were detected on all 10 maize chromosomes, they were not evenly distributed throughout the genome. QTL for associated traits can tend to cluster in certain regions probably because these regions contain QTL or genes with pleiotropic effects or tightly linked QTL influencing different traits [38,39]. Herein, we found 57 QTL clustered into 21 hotspots (QC, QTL cluster) and the associated genes are listed in Table 2. For example, the familiar maize flowering time genes *ZCN8* and *ZmCCT* were included in QC15 and QC19, respectively [3,22]. The most stable QTL, *qDTT8-1*, was identified in nine single environments and under MPD during single-plant density analysis. The Qi 319 allele at *qDTT8-1* causes tasseling to occur earlier and the additive effects of this QTL increase with plant density. *qDTS8* and *qDTP8-1* were anchored in QC14 with *qDTT8*-1, and the alleles at these loci from Qi 319 all promoted flowering (Table 2; Table S3). A QTL for plant height overlapped with *qDTT8-1* and the allele derived from Qi 319 increased plant height (data not shown). These effects are similar to the effects of *GIGANTEA1* (*GI1*), which is in the confidence

interval of *qDTT8-1* [13]. Thus, we speculate that *GI1* is a candidate gene for *qDTT8-1* and, if so, might be useful for reducing the prolongation of the growth period of maize under high plant density. The stable QTL *qDTT10-4* and *qDTP10-5* were contained in QC21 together with *qDTS10* and *qTAI10*-6. The positive effects of all these QTL suggested that the allele from Qi 319 delays flowering time (Tables 2; Table S3). The secondary traits ASI and TAI comprise two separate primary traits, reflecting a common genetic basis for their component traits. The QTL for secondary traits showed low stability in different genetic backgrounds and environments, and the mapped locations of QTL for ASI and TAI often overlapped with the locations of QTL for their component traits (Fig. 2; Tables S3 and S6). The locations of QTL for all secondary traits clustered with those influencing at least one of their component traits. For instance, six QCs contained DTT, DTP, and TAI (Table 2). No single QC contained QTL for all five flowering time-related traits, indicating the complexity and dissimilarity of the genetic bases of maize flowering time (Table 2). These flowering time-related traits had not only common genetic bases but also independent regulatory pathways among associated traits.

CRediT authorship contribution statement

Xinhai Li, Wenying Zhang, Jianfeng Weng and Liwei Wang conceived and designed the experiments. Baoqiang Wang, Wei Song, Xinghua Li, Quanguo Zhang, and Liwei Wang performed the field experiments. Zhiqiang Zhou and Jianfeng Weng performed genotyping and constructed the bin map. Liwei Wang and Zhiqiang Zhou performed the statistical analysis and QTL analysis. Liwei Wang, Ronggai Li, Zhiqiang Zhou, and Jianfeng Weng discussed and drafted the manuscript. All authors read and approved the final manuscript. Xinhai Li and Wei Song should be considered co-corresponding authors.

Declaration of competing interest

The authors declare that they have no known competing financial interests or personal relationships that could have appeared to influence the work reported in this paper.

Acknowledgments

This study was supported by Hebei Province Special Postdoctoral Financial Assistance (B2017003030), the Youth Innovation Fund of the Institute of Cereal and Oil Crops, Hebei Academy of Agriculture and Forestry Sciences (LYS2017001), the Hebei Financial Special Project: Construction of Talents Team for Agricultural Science Technical Innovation, and the China Agriculture Research System (CARS-02).

Appendix A. Supplementary data

Supplementary data for this article can be found online at https://doi.org/10.1016/j.cj.2020.07.009.

References

[1] M. Liu, X. Tan, Y. Yang, P. Liu, X. Zhang, Y. Zhang, L. Wang, Y.u. Hu, L. Ma, Z. Li, Y. Zhang, C. Zou, H. Lin, S. Gao, M. Lee, T. Lübberstedt, G. Pan, Y. Shen, Analysis of the genetic architecture of maize kernel size traits by combined linkage and association mapping, Plant Biotechnol. J. 18 (2020) 207–221.

[2] E.S. Buckler, J.B. Holland, P.J. Bradbury, C.B. Acharya, P.J. Brown, C. Browne, E. Ersoz, S. Flint-Garcia, A. Garcia, J.C. Glaubitz, M.M. Goodman, C. Harjes, K. Guill, D.E. Kroon, S. Larsson, N.K. Lepak, H. Li, S.E. Mitchell, G. Pressoir, J.A. Peiffer, M. O. Rosas, T.R. Rocheford, M.C. Romay, S. Romero, S. Salvo, H.S. Villeda, H. Sofia da Silva, Q. Sun, F. Tian, N. Upadyayula, D. Ware, H. Yates, J. Yu, Z. Zhang, S. Kresovich, M.D. McMullen, The genetic architecture of maize flowering time, Science 325 (2009) 714–718.

[3] L. Guo, X. Wang, M. Zhao, C. Huang, C. Li, D. Li, C. Yang, A.M. York, W. Xue, G. Xu, Y. Liang, Q. Chen, J.F. Doebley, F. Tian, Stepwise *cis*-regulatory changes in *ZCN8* contribute to maize flowering-time adaptation, Curr. Biol. 28 (2018) 3005–3015.

[4] C. Huang, H. Sun, D. Xu, Q. Chen, Y. Liang, X. Wang, G. Xu, J. Tian, C. Wang, D. Li, L. Wu, X. Yang, W. Jin, J.F. Doebley, F. Tian, *ZmCCT9* enhances maize adaptation to higher latitudes, PNAS 115 (2018) E334–E341.

[5] R. Shrestha, J. Gómezariza, V. Brambilla, F. Fornara, Molecular control of seasonal flowering in rice, *Arabidopsis* and temperate cereals, Ann. Bot. 114 (2014) 445.

[6] M. Blümel, N. Dally, C. Jung, Flowering time regulation in crops–what did we learn from *Arabidopsis*?, Curr. Opin. Biotechnol. 32 (2015) 121–129.

[7] Y. Li, C. Li, P.J. Bradbury, X. Liu, F. Lu, C.M. Romay, J.C. Glaubitz, X. Wu, B.o. Peng, Y. Shi, Y. Song, D. Zhang, E.S. Buckler, Z. Zhang, Y.u. Li, T. Wang, Identification of genetic variants associated with maize flowering time using an extremely large multi-genetic background population, Plant J. 86 (2016) 391–402.

[8] P.K. Boss, R.M. Bastow, J.S. Mylne, C. Dean, Multiple pathways in the decision to flower: enabling, promoting, and resetting, Plant Cell 16 (2004) S18–S31.

[9] I. Ausin, C. Alonso-Blanco, J.-M. Martinez-Zapater, Environmental regulation of flowering, Int. J. Dev. Biol.. 49 (2005) 689–705.

[10] X. Wang, L. Wu, S. Zhang, L. Wu, L. Ku, X. Wei, L. Xie, Y. Chen, Robust expression and association of *ZmCCA1* with circadian rhythms in maize, Plant Cell Rep. 30 (2011) 1261–1272.

[11] P. Alter, S. Bircheneder, L.-Z. Zhou, U. Schlüter, M. Gahrtz, U. Sonnewald, T. Dresselhaus, Flowering time-regulated genes in maize include the transcription factor ZmMADS1, Plant Physiol. 172 (2016) 389–404.

[12] M. Jin, X. Liu, W. Jia, H. Liu, W. Li, Y. Peng, Y. Du, Y. Wang, Y. Yin, X. Zhang, Q. Liu, M. Deng, N. Li, X. Cui, D. Hao, J. Yan, *ZmCOL3* , a CCT gene represses flowering in maize by interfering with the circadian clock and activating expression of ZmCCT: maize CCT genes and flowering time, J. Integr. Plant Biol. 60 (2018) 465–480.

[13] Claire Bendix, Juan M. Mendoza, Desiree N. Stanley, Robert Meeley, Frank G. Harmon, The circadian clock-associated gene gigantea1 affects maize developmental transitions: gigantea1 regulates maize developmental transitions, Plant Cell Environ. 36 (2013) 1379–1390.

[14] M.G. Muszynski, T. Dam, B. Li, D.M. Shirbroun, Z. Hou, E. Bruggemann, R. Archibald, E.V. Ananiev, O.N. Danilevskaya, *Delayed flowering1* encodes a basic leucine zipper protein that mediates floral inductive signals at the shoot apex in maize, Plant Physiol. 142 (2006) 1523–1536.

[15] J. Colasanti, R. Tremblay, A.Y. Wong, V. Coneva, A. Kozaki, B.K. Mable, The maize *INDETERMINATE1* flowering time regulator defines a highly conserved zinc finger protein family in higher plants, BMC Genomics 7 (2006) 158.

[16] O.N. Danilevskaya, X. Meng, D.A. Selinger, S. Deschamps, P. Hermon, G. Vansant, R. Gupta, E.V. Ananiev, M.G. Muszynski, Involvement of the MADS-box gene *ZMM4* in floral induction and inflorescence development in maize, Plant Physiol. 147 (2008) 2054–2069.

[17] C. Zhang, Z. Zhou, H. Yong, X. Zhang, Z. Hao, F. Zhang, M. Li, D. Zhang, X. Li, Z. Wang, J. Weng, Analysis of the genetic architecture of maize ear and grain morphological traits by combined linkage and association mapping, Theor. Appl. Genet. 130 (2017) 1011–1029.

[18] D. Li, X. Wang, X. Zhang, Q. Chen, G. Xu, D. Xu, C. Wang, Y. Liang, L. Wu, C. Huang, J. Tian, Y. Wu, F. Tian, The genetic architecture of leaf number and its genetic relationship to flowering time in maize, New Phytol. 210 (2016) 256–268.

[19] S. Salvi, R. Tuberosa, E. Chiapparino, M. Maccaferri, S. Veillet, L.V. Beuningen, P. Isaac, K. Edwards, R.L. Phillips, Toward positional cloning of *Vgt1*, a QTL controlling the transition from the vegetative to the reproductive phase in maize, Plant Mol. Biol. 48 (2002) 601–613.

[20] Y. Liang, Q. Liu, X. Wang, C. Huang, G. Xu, S. Hey, H. Lin, C. Li, D. Xu, L. Wu, C. Wang, W. Wu, J. Xia, X. Han, S. Lu, J. Lai, W. Song, P.S. Schnable, F. Tian, *ZmMADS69* functions as a flowering activator through the *ZmRap2.7-ZCN8* regulatory module and contributes to maize flowering time adaptation, New Phytol. 221 (2018) 2335–2347.

[21] S. Ducrocq, C. Giauffret, D. Madur, V. Combes, F. Dumas, S. Jouanne, D. Coubriche, P. Jamin, L. Moreau, A. Charcosset, Fine mapping and haplotype structure analysis of a major flowering time quantitative trait locus on maize chromosome 10, Genetics 183 (2009) 1555–1563.

[22] H. Hung, L.M. Shannon, F. Tian, P.J. Bradbury, C. Chen, S.A. Flint-Garcia, M.D. McMullen, D. Ware, E.S. Buckler, J.F. Doebley, J.B. Holland, *ZmCCT* and the genetic basis of day-length adaptation underlying the postdomestication spread of maize, Proc. Natl. Acad. Sci. U.S.A. 109 (2012) E1913–E1921.

[23] S. Hokmalipour, R. Seyedsharifi, S. Jamaatiesomarin, M. Hassanzadeh, M. Shiriejanagard, R. Zabihiemahmoodabad, Evaluation of plant density and nitrogen fertilizer on yield, yield components and growth of maize, World Appl. Sci. J. (2010) 1157–1162.

[24] J. Guo, Z. Chen, Z. Liu, B. Wang, W. Song, W. Li, J. Chen, J. Dai, J. Lai, Identification of genetic factors affecting plant density response through QTL mapping of yield component traits in maize (*Zea mays* L.), Euphytica 182 (2011) 409–422.

[25] A. Sher, A. Khan, L. Cai, M.I. Ahmad, U. Asharf, S.A. Jamoro, Response of maize grown under high plant density; performance, issues and management-a critical review, Adv. Crop Sci. Technol. 5 (2017) 275.

[26] Y. Assefa, P. Carter, M. Hinds, G. Bhalla, R. Schon, M. Jeschke, S. Paszkiewicz, S. Smith, I.A. Ciampitti, Analysis of long term study indicates both agronomic optimal plant density and increase maize yield per plant contributed to yield gain, Sci. Rep. 8 (2018) 4937.

[27] G.O. Edmeades, N.A. Fairey, T.B. Daynard, Influence of plant density on the distribution of ^{14}C-labelled assimilate in maize at flowering, Can. J. Plant Sci. 59 (1979) 577–584.
[28] J. Ma, D. Zhang, Y. Cao, L. Wang, J. Li, T. Lübberstedt, T. Wang, Y. Li, H. Li, Heterosis-related genes under different planting densities in maize (*Zea mays* L.), J. Exp. Bot. 69 (2018) 5077–5087.
[29] Z. Zhou, C. Zhang, X. Lu, L. Wang, Z. Hao, M. Li, D. Zhang, H. Yong, H. Zhu, J. Weng, X. Li, Dissecting the genetic basis underlying combining ability of plant height related traits in maize, Front. Plant Sci. 9 (2018) 1117.
[30] Z. Zhou, C. Zhang, Y. Zhou, Z. Hao, Z. Wang, X. Zeng, H. Di, M. Li, D. Zhang, H. Yong, S. Zhang, J. Weng, X. Li, Genetic dissection of maize plant architecture with an ultra-high density bin map based on recombinant inbred lines, BMC Genomics 17 (2016) 178.
[31] L.A. Kirkpatrick, B.C. Feeney, A Simple Guide to IBM SPSS: for Version 22.0, Wadsworth Publishing, Belmont, California, USA, 2014.
[32] L. Meng, H. Li, L. Zhang, J. Wang, QTL IciMapping: Integrated software for genetic linkage map construction and quantitative trait locus mapping in biparental populations, Crop J. 3 (2015) 269–283.
[33] S.J. Knapp, W.W. Stroup, W.M. Ross, Exact confidence intervals for heritability on a progeny mean basis, Crop Sci. 25 (1985) 192–194.
[34] H. Li, G. Ye, J. Wang, A modified algorithm for the improvement of composite interval mapping, Genetics 175 (2007) 361–374.
[35] Christian Jung, Andreas E. Müller, Flowering time control and applications in plant breeding, Trends Plant Sci. 14 (2009) 563–573.
[36] C. Joseph, C. Viktoriya, Mechanisms of floral induction in grasses: something borrowed, something new, Plant Physiol. 149 (2009) 56–62.
[37] C. Bendix, C. Marshall, F. Harmon, Circadian clock genes universally control key agricultural traits, Mol. Plant 8 (2015) 1135–1152.
[38] Y. Liu, L. Wang, C. Sun, Z. Zhang, Y. Zheng, F. Qiu, Genetic analysis and major QTL detection for maize kernel size and weight in multi-environments, Theor. Appl. Genet. 127 (2014) 1019–1037.
[39] C. Yang, D. Tang, J. Qu, L. Zhang, L. Zhang, Z. Chen, J. Liu, Genetic mapping of QTL for the sizes of eight consecutive leaves below the tassel in maize (*Zea mays* L.), Theor. Appl. Genet. 129 (2016) 2191–2209.